



J. Serb. Chem. Soc. 91 (3) 303–316 (2026)
JSCS–5493

Removal of Pb(II), Cd(II) and Zn(II) from landfill soil and leachate using a graphene oxide membrane

DRAGANA STEVIĆ^{1*}, SUNČICA SUKUR², RADOVAN KUKOBAT³, SUZANA GOTOVAC ATLAGIĆ², PREDRAG ILIĆ⁴, FRANCESCO SIRIO FUMAGALLI⁵, ANDREA VALSESIA⁵, PASCAL COLPO⁵ and SVETLANA POPOVIĆ^{1**}

¹Faculty of Technology Novi Sad, University of Novi Sad, Boulevard cara Lazara 1, Novi Sad, Serbia, ²Faculty of Natural Sciences and Mathematics, Department of Chemistry, University of Banja Luka, Mladena Stojanovića 2, 78000, Banja Luka, the Republic of Srpska, Bosnia and Herzegovina, ³Faculty of Technology, Department of Chemical Engineering and Technology, University of Banja Luka, B.V Stepe Stepanovića 73, Banja Luka, the Republic of Srpska, Bosnia and Herzegovina, ⁴Institute for Protection and Ecology of the Republic of Srpska, Banja Luka, Bosnia and Herzegovina and ⁵European Commission, Joint Research Centre (JRC), Ispra, Italy

(Received 5 May, revised 27 June, accepted 29 October 2025)

Abstract: Since rainwater extracts toxic metals from landfills, creating harmful leachate, developing methods to remove these metals is necessary. This work presents a method of toxic metal ions removal from a loam-type soil consisting of washing the soil with a mild washing agent to extract toxic metals in a leachate, and a purification of the leachate by filtering it through a synthesized graphene oxide (GO) membrane. As washing agents, the pure water and a mild solution of HCl (0.01 M) were tested. The GO membrane was synthesized using natural Madagascar graphite. The solution of HCl showed a significantly higher washing efficiency of Zn(II), Cd(II) and Pb(II) cations than pure water due to its acidic nature. An intrinsic GO membrane with an interlayer distance of 0.68–0.74 nm (before and after filtration) and a thickness of ~0.70 μm yielded rejections of 99.80, 96.15 and 44.00 % for Pb(II), Cd(II) and Zn(II) ions, respectively. Molecular dynamics simulation showed that ions retained in the GO interfaces due to the narrow interlayer distance, leading to membrane fouling. Nevertheless, the high rejections of Pb(II) and Cd(II) support the possibility of purifying landfill soil leachate by the GO membrane.

Keywords: landfill soil; washing; cations; graphene oxide; membrane.

*,** Corresponding authors. E-mail: (*)dragana.stevic05@gmail.com, (**)svetlana.popovic@uns.ac.rs
<https://doi.org/10.2298/JSC250505079S>



INTRODUCTION

Soil contamination by metals in landfills poses a significant global problem. Since the Industrial Revolution, the presence of metal contaminants in soil has steadily increased due to a range of human activities, including manufacturing, coal combustion, petrochemical spills, atmospheric deposition, mining, waste disposal, wastewater irrigation, the use of agrochemicals (such as pesticides and fertilizers) and soil amendments.¹ Recent studies indicate that metal concentrations in soil are already reaching critical levels, with some approaching or exceeding agricultural threshold values of 14–17 %.² Certain metals, such as cadmium and arsenic, can accumulate in food crops at concentrations that are unsafe for human consumption.² Hazardous waste landfills are notable sources of toxic metals, including lead, arsenic, chromium, cadmium, zinc, cobalt and nickel, all of which have been detected as common soil contaminants in such areas.³ Waste decomposes over time in the presence of infiltrated water, forming a dark liquid called leachate.⁴ This leachate leaks from the landfill into the surrounding soil, contaminating ecosystems.⁵ Over time, it migrates through the soil layers, leading to severe and persistent pollution.⁶ Given these risks, the contamination of landfill soils with metals represents a critical environmental challenge that must be addressed to ensure a sustainable future.

Researchers have been actively working on finding new methods for soil remediation and consequent metal removal from contaminated water. Most of the scientific papers deal with soil washing using acids of a bit higher concentration, such as 3 M HCl to remove Cd or a mixture of 0.6 M H₂SO₄ and 0.6 M H₃PO₄ to remove As, Cu, Pb and Zn.^{7,8} These methods reach high removal efficiencies, but the soil remains acidic with low production potential. Hence, methods for mild and environmentally friendly landfill soil and leachate treatments are yet to be developed.

Treating washing leachate that contains toxic metals is essential to prevent secondary pollution. Membrane technology for metal ion removal is efficient and has advantages over other methods because of its low energy consumption, environmentally friendly nature, compact design, and scalability.⁹ GO membranes are atomically thin and have interlayers that act as natural nanopores for ion separation.¹⁰ Other membrane materials, such as polymers, MOFs, zeolites, MXenes, their composites and mixed-matrix membranes could also be used for ionic separation.¹¹ These membranes have large pores and cracks that are not suitable for ionic separations, while polymer and mixed-matrix membranes offer high efficiency but low water permeance. On the other hand, GO-based membranes have been widely studied for metal ion filtration in water desalination.¹² To the best of our knowledge, the integrated approach involving landfill soil washing followed by leachate filtration has not yet been documented in the existing literature. While

graphene oxide (GO) membranes have been extensively studied for metal ion removal in various aqueous systems, their application in the treatment of landfill leachate remains underexplored.

This work presents an efficient and environmentally friendly method for soil washing and subsequent leachate membrane filtration. Thus, as mild and environmentally friendly washing agents, pure water and a 0.01 M HCl solution were tested for washing the landfill soil. Further, the novelty of this research lies in using an intrinsic graphene oxide (GO) membrane for leachate filtration and employing molecular dynamics simulation to understand the mechanism of retention. Thus, the objectives of this work are the development of an environmentally friendly landfill soil washing method, the subsequent use of a GO membrane for landfill soil wastewater purification, and elucidation of the metal ion filtration mechanism. The aim is to examine the effectiveness of soil washing with water and diluted acid for future practical implementation, as the simple preparation of an intrinsic GO membrane via vacuum filtration makes the overall method desirable for future application.

EXPERIMENTAL

Landfill soil treatment

Soil from the “Cicanovic Forest”, landfill near the Bijeljina region in Bosnia and Herzegovina, was collected from the surface at one location and preserved in a fridge at 5 °C, for the experiments. The jar test method was used to determine the type of soil.¹³ A jar was filled with soil up to a third of its volume, and filled with 10 g of detergent and water. The mixture was shaken, and the heights of the sand, silt, and clay layers were measured after 1 min, 2, and 48 h, respectively (Fig. S-1 of the Supplementary material to this paper). The soil composition of 12.5 % clay, 37.5 % silt and 50 % sand according to the soil texture pyramid, was determined to be a loam type of soil.¹⁴

Pure water and a 0.01 M solution of HCl (prepared from concentrated HCl of analytical purity grade, purchased from Sigma–Aldrich) were used as washing agents. As acidification of soil can affect plant health and productivity,¹⁵ we have used a low concentration of HCl for soil washing to minimize the decrease of the pH and to simulate environmental conditions. The washing process involved mixing of 20 g of soil with 150 mL of H₂O or 0.01M HCl and exposing the mixture to the sonication in an ultrasonic bath (Bandelin, DT 102H, Germany) at a frequency of 50 kHz and a power of 150 W for 15, 30, 45, 60 and 120 min at room temperature so to enhance extraction of metals by breaking the soil aggregates. Samples were then filtered to obtain leachates for further treating by membrane filtration.

Graphene oxide (GO) membrane preparation and leachate filtration

GO was prepared from natural Madagascar graphite using a modified Hummers' method.¹⁶ A dispersion of GO (10 mL) at a concentration of 0.001 wt. % was filtered through a polytetrafluoroethylene membrane (Omnipore, 5 µm PTFE membrane, 47 mm diameter). A thin GO membrane was formed after 2 h of filtration at a pressure of 8×10^4 Pa (Fig. S-2a of the Supplementary material). The leachate containing toxic metals (10 mL) was filtered through the GO membrane at a vacuum of 8×10^4 Pa (0.8 bar, Fig. S-2b of the Supplementary material). The metal ion composition in the permeated water was then analysed.

The membrane's thickness was estimated from the density and mass of the GO membrane on the polytetrafluoroethylene (PTFE) substrate. A GO membrane with a mass of 1 mg on a PTFE substrate (19.625 cm² with a membrane diameter of 5 cm) has a thickness of ~0.7 μm, considering the density of GO at room temperature (0.75 g cm⁻³)¹⁷.

Materials characterizations

A Fourier transform infrared (FTIR) spectrophotometer with attenuated total reflectance (ATR-S, IR Spirit Shimadzu, Japan) was used for soil characterization before and after washing. A Raman spectrophotometer (Renishaw, UK), equipped with lasers of λ 532 and 780 nm, was used with a grid resolution of 1200 lines/cm and an integration time per pixel of 5 s. A 100× magnification objective with a numerical aperture of 1.25 was used. Cosmic Ray Removal and baseline correction tools were applied to the spectra before univariate analysis.

A X-ray diffraction (XRD) system (Bruker, Cu K-alpha, λ = 1.5406 Å, X-ray lamp power 1600 W, I = 40 mA and U = 40 kV) was used to characterize the GO membrane before and after water filtration. A Göbel mirror, a 2.5° soller, and a 0.3 mm pinhole were inserted along the primary beam path. A 0.6 mm slit and a 2.5° soller were mounted on the secondary beam path. The 2θ range was from 6 to 90°, with a step size of 0.01° and an integration time per step of 3 s. The surface morphology of the membrane, both before and after water filtration, was characterized using a scanning electron microscope (SEM, JEOL JSM-7800F FESEM, France). The instrument was equipped with an in-lens thermal field emission gun with a Schottky emitter (W-filament). The accelerating voltage was 5 kV, and the probe current was 10 pA. The detector used was an in-chamber Everhart-Thornley SE detector or a lower electron detector (LED).

The ionic conductivity (Hanna, EC 214 Conductivity Meter) and pH (Hanna, pH 211 microprocessor pH meter) were measured in the samples before and after soil washing. A UV–Vis spectrophotometer (UV-1800, Shimadzu, Japan) was used to measure the optical absorbance spectra of the water before and after filtration through the GO membrane. An atomic absorption spectrometer (Perkin Elmer Analyst 400, USA) was used to measure the metal ion concentrations in the water for the future estimation of ion rejection by the membrane.

The rejection percentage of metal ions separated by the GO membrane was calculated using the following expression:

$$\text{Rejection} = 100\left(1 - \frac{c_p}{c_f}\right) \quad (1)$$

where c_f is the concentration of a component in the feed (mg kg⁻¹), and c_p is the concentration of ions in permeate (mg kg⁻¹).

Computational details

Molecular dynamics simulations were performed using the large-scale atomic/molecular massively parallel simulator (LAMMPS)¹⁸ to investigate the ion separation mechanism through the GO membrane. The simulation model consisted of two graphene layers with nanowindows, along with water molecules containing Pb(II), Cd(II) and Zn(II) ions in chloride form to maintain overall charge neutrality. Snapshots were visualized using DS Visualizer.

The GO–GO interlayer distances in the model were varied to be 0.33, 0.40, 0.50, 0.60, 0.70, and 0.90 nm. Circular nanowindows were created on the basal planes of the graphene, applying periodic boundary conditions along the *X* and *Y* axes, while the *Z* axis was defined as a repulsive wall. The simulation box dimensions (in Å) were set as follows: *X*, –12.31175 to 12.31175; *Y*, –34.104 to 34.104 and *Z*, –150 to 50, with the graphene layers at the center of the coordinate system.

Simulations were carried out in the NVT ensemble, with temperature regulated by the Nosé–Hoover thermostat. The SPC/E¹⁹ water model was employed, and charges for the Pb(II) cations and Cl(I) anions were assigned using the Lennard–Jones (LJ) parameters given in Table S-I of the Supplementary material. A timestep was 1 fs. By varying the interlayer distance, the model evaluated the potential permeance of metal ions through the GO membrane.

RESULTS AND DISCUSSION

Washing of the metal cations of Cd(II), Zn(II) and Pb(II) from landfill soil

Throughout the washing process, both washing agents, *i.e.*, pure water and 0.01 M HCl solution, proved to extract the toxic metals into the landfill wastewater (Fig. 1a and b). The 0.01 M HCl yielded higher percentages of toxic metal cations extraction from the landfill soil than H₂O, likely due to the acidic nature of HCl, which facilitates the dissolution of metals and the formation of metal cations. The landfill soil washing with diluted HCl is the most efficient for Cd (7.58 %), while the removal percentages for Pb and Zn were lower (Table S-II of the Supplementary material). Metal cations diffuse through the soil particles, reaching the outer surface and forming leachate that should be further purified to avoid secondary pollution.

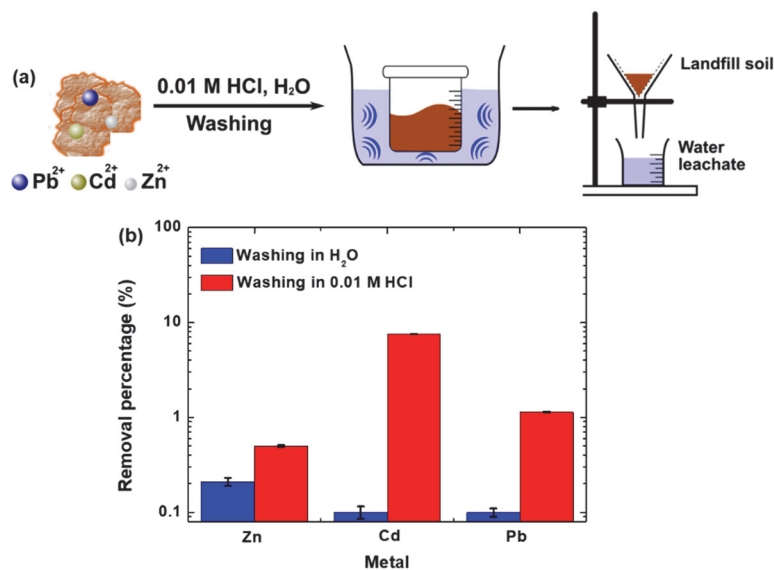


Fig. 1. Landfill soil washing. a) Washing procedure with 0.01 M HCl and H₂O. b) Removal percentage of Zn (II), Cd (II) and Pb (II) cations after ultrasonication.

Surface functional groups on the landfill soil before and after washing

The landfill soil, composed of sand, silt, and clay, also contains Si in the structure. FTIR spectra of the soil washed with H₂O and 0.01 M HCl show a

distinct band at $\sim 1000\text{ cm}^{-1}$ from stretching vibrations of the Si–O group,²⁰ and a band at $\sim 3500\text{ cm}^{-1}$ from the O–H group in water adsorbed in the soil (Fig. 2 and Figs. S-3 and S-4 of the Supplementary material). The Si–O band is slightly shifted to a lower frequency region after washing with H₂O and 0.01 M HCl, which could be due to possible interactions of H⁺ with active sites on the Si–O band (Fig. 2). The Si–O bands of the soil after washing with H₂O and 0.01 M HCl became narrower, and the absolute peak area decreased from 182 to 135 cm⁻¹. The decrease in the Si–O absorption peak area is likely from the removal of vibrational fragments that follow the primary Si–O vibration. The small band at $\sim 1300\text{ cm}^{-1}$ could be assigned to metal–oxygen (Me–O) vibrations in the loam. This Me–O vibrational band disappears after washing with H₂O and 0.01 M HCl, which is attributed to the removal of metal from the soil.

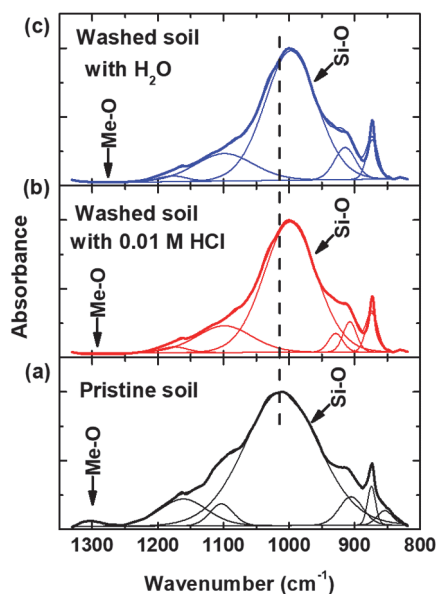


Fig. 2. FTIR spectra of the Si–O band in loam-type soil. a) Pristine soil. b) Soil washed with 0.01 M HCl for 60 min. c) Soil washed with H₂O.

Ionic conductivity of the leachate

Metal ions dissolved from the soil increased the electrical conductivity of the landfill leachate (Fig. S-5 of the Supplementary material). The electrical conductivity of the soil dissolved in 0.01 M HCl and H₂O increased to ~ 1800 and $\sim 600\ \mu\text{S cm}^{-1}$, respectively. The electrical conductivity shows an increasing tendency with washing time due to the evolution of ions from the soil, while the pH remains constant and nearly neutral because of the absence of acidic or basic ions in the leachate (Fig. S-5). An increase in the electrical conductivity was anticipated due to the evolved Pb(II), Cd(II) and Zn(II) cations. These metal cations in leachate

were separated using the GO membrane, as will be further discussed from experimental and the GO structure modelling results.

Purification of leachate using an intrinsic GO membrane

Separation of toxic metal cations from a leachate was conducted using an $\sim 0.70 \mu\text{m}$ thick GO membrane (Fig. 3a–c). The rejection of metal ions by the GO membrane increases with the metal ion hydrated diameter (Fig. 3d). The ionic diameter depends on the number of ligands surrounding the ions, having an increasing tendency in the order of $\text{Zn(II)} < \text{Cd(II)} < \text{Pb(II)}$ cations. Metal ions and molecules can diffuse through nano-windows or defects on graphene-like surfaces, being transferred through the interlayers of GO. The Pb(II) and Cd(II) cations have difficulty permeating between the layers of GO because of the narrow effective width at the GO–GO interfaces, giving rejection as high as $\sim 100\%$. Zn(II) cations have a smaller ionic diameter than the GO interlayer distance, permeating between the GO layers at a relatively low rejection of $\sim 40\%$. High cation rejection can be assigned to the stacking of GO layers under vacuum. The thin membrane was produced to ensure rapid water filtration through the membrane. The water permeance during metal cation separation shows a decreasing tendency against time from $20.3 \text{ L m}^{-2} \text{ h}^{-1} \text{ bar}^{-1}$ after 0 h to $7.8 \text{ L m}^{-2} \text{ h}^{-1} \text{ bar}^{-1}$ after 4 h (Fig. S-6 of the Supplementary material). The decrease in water permeance occurs due to membrane foul-

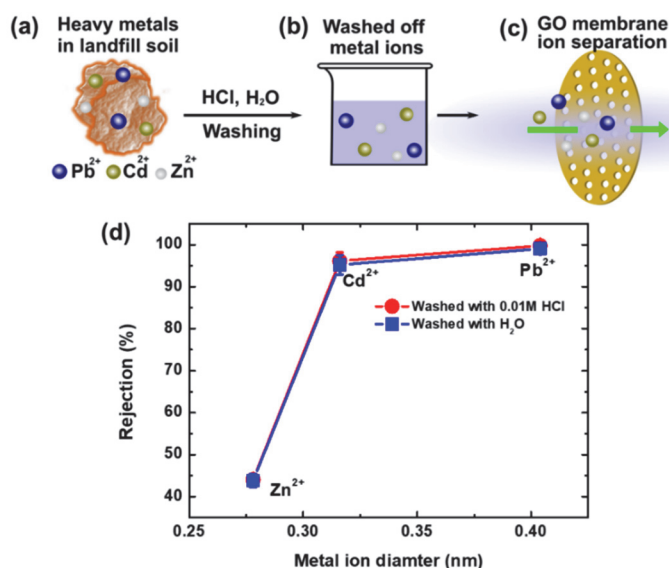


Fig. 3. Toxic metals from landfill soil and their separation. a) Landfill soil contaminated with toxic metals. b) Water containing metal cations of Pb(II) , Cd(II) and Zn(II) . c) Separation of toxic metals through the GO membrane. d) Rejection of metal cations in 0.01 M HCl and water against their size.

ing. The leachate contains a small quantity of suspended soil particles, which remain on the membrane surface as evidenced by a decrease in the UV–Vis spectra before and after filtration (Fig. S-7 of the Supplementary material).

The structure of the GO membrane before and after leachate filtration

The GO membrane on the PTFE support, produced by vacuum filtration (Fig. S-2), has a layer-like structure. The membrane is composed of GO layers stacked together, forming a compact structure (Fig. 4a₁ and b₁). GO layers have a lateral size of $\sim 0.7 \mu\text{m}$,²¹ covering the surface of the porous PTFE support. The surface morphology of the GO membrane changed slightly after filtering the landfill water contaminated with metal cations (Fig. 4a₂ and b₂). This can be attributed to the deposition of contaminants onto the GO membrane surface. The GO membrane, both before and after metal cation separation, has a flat surface morphology due to the uniform and flat PTFE substrate on the rigid vacuum filter support. The membrane has a compact structure without cracks, which is important for the future large-scale production of crack-free membranes for landfill cation separation.

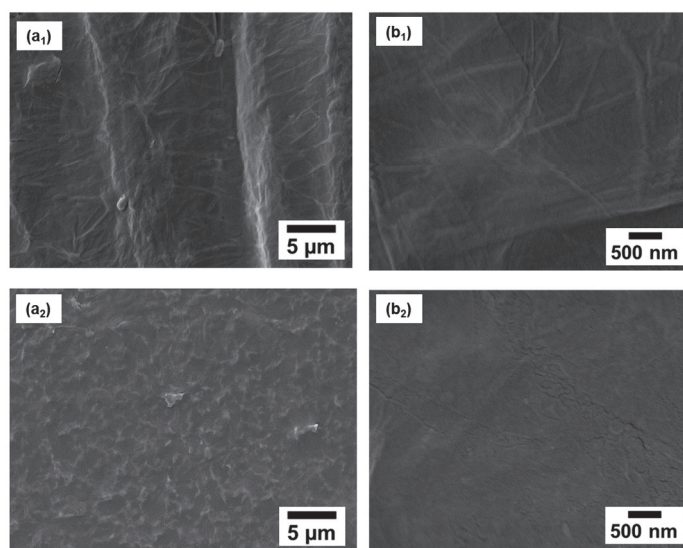


Fig. 4. SEM micrographs of the GO membrane before and after filtration of 10 mL of landfill water contaminated with metal cations; a₁ and b₁: low and high magnification of the membrane before filtration; a₂ and b₂: low and high magnifications of the membrane after filtration. The low and high magnifications were used for better understanding the membrane surface.

The interlayer distance of the GO–GO was examined from XRD patterns in the two-theta region of 8 to 37°. The GO diffraction peak from the (002) crystal plane and the bands from defective GO are prominent both before and after metal

ion filtration (Fig. 5a and b). The absolute intensity of the GO bands decreased after water filtration, which is likely due to the deposition of soil particles onto the surface of the GO membrane. The small soil particles that cause the turbidity of the soil dispersion were separated by filtration through the GO membrane, as confirmed by a decrease in the optical absorbance intensity in the UV–Vis region of 220–500 nm (Fig. S-6 of the Supplementary material). After metal ion separation, the intensity of the XRD peaks decreased, and the position of the (002) band shifted from 12.50 to 11.86° (2θ) due to an increase in the interlayer distance. According to Bragg's law ($2d\sin\theta = \lambda$),²² the interlayer distance d increased from 0.70 to 0.74 nm. This increase is likely due to the intercalation of water and metal ions into the GO–GO interlayer space.²³ Fortunately, this increase in the interlayer distance is insignificant, which contributes to stable ion separation over time.

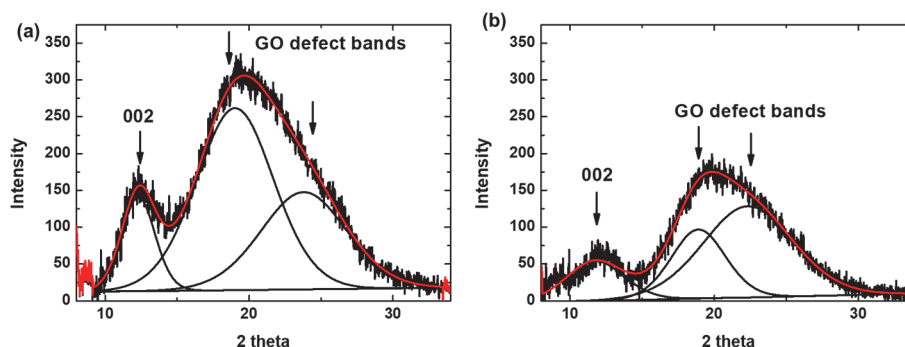


Fig. 5. XRD patterns of GO membranes. a) GO membrane before cation separation; b) GO membrane after ion separation.

The crystallinity of GO membranes before and after ion filtration was examined using Raman spectroscopy with a laser wavelength of 532 nm. Defects were created in the GO during the exfoliation process, and the edges of these defects (referred to as nanowindows) can be identified by oxygen functional groups such as carboxyl, carbonyl, hydroxyl and epoxy.²⁴ The GO membrane has a prominent G-band from crystalline sp^2 carbon atoms that vibrate in-plane and a D-band from defective sp^3 carbon atoms that are bound with oxygen functional groups (Fig. 6). Metal ions permeate through the GO nanowindows, which are a few nanometers in size.²⁵ The GO membrane is highly defective, as indicated by a high value of $I_{D/G} = 0.96$. After metal ion permeance, the D-band intensity ratio slightly increased to $I_{D/G} = 0.99$, suggesting an increase in the defects of GO. The slight shift in the G-band suggests the presence of charge transfer interactions between metal cations of Zn(II), Cd(II) or Pb(II) and graphene. Electron charge transfer interactions between unhybridized p_z electrons of sp^2 carbon atoms and d-states of metal cations should occur,²⁶ leading to the shift in the G-band of GO. The metal ions

could be trapped on the basal plane of GO and in between the layers, leading to the metal ion separation.

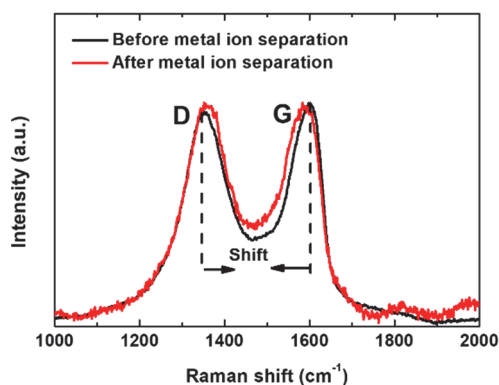


Fig. 6. Raman spectra of the GO membrane recorded at a laser wavelength of 532 nm. The spectra of the GO membranes were recorded before water filtration (black line) and after water filtration (red line).

Metal ion separation mechanism

The mechanism of toxic metal cations retention by GO membrane was modelled using MD simulations. The GO membrane model of two layers served for examination of the ion separation mechanism (Fig. 7). The GO layers have

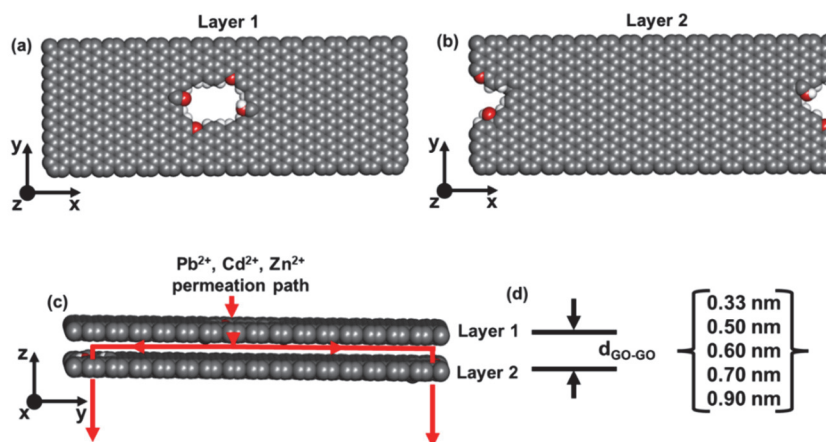


Fig. 7. A unit cell of the GO membrane models with the periodic boundary conditions for molecular dynamics simulation of Pb(II), Cd(II) and Zn(II) cation permeance. a) GO layer 1 with nano-windows of ~1 nm in diameter. b) GO layer 2 with nano-windows of ~1 nm in diameter. c) GO layers with denoted permeance paths for metal ions between the GO layers through the nano-windows. d) Internuclear distances between GO layers used for MD simulations of metal cation permeance.

nano-windows on the basal planes, serving for examination of the ion separation mechanism between the layers (Fig. 7a and b). The metal ions can enter the nano-windows on the basal planes and penetrate between the layers of GO at the interlayer distances of 0.33–0.90 nm (Fig. 7c). The rejection of metal ions by the GO layered membrane depends on the interlayer distance. Ions can freely enter the nano-windows on GO, whose size can reach nearly ~ 1 nm²⁷ in diameter. The sizes of the nano-windows on GO cannot be precisely controlled during synthesis. Given that these nano-windows are substantially larger than the metal ions, the interlayer spacing probably constitutes the primary barrier to metal ion rejection.²⁸ Adjusting the interlayer distance from the completely stacked GO layers at the distance of 0.33 nm to a distance larger than the sizes of the metal ions should lead to ion separation performances that are similar to the experimental results.

The GO membrane with an interlayer distance of 0.33 nm is impermeable to metal ions due to the narrow gap, which leads to their complete exclusion (Fig. S-8 of the Supplementary material). The GO membrane with an interlayer distance of 0.50 nm is permeable to Cd(II) and Zn(II) cations (Fig. S-8), but is impermeable to Pb(II) cations, resulting in their complete rejection (100 %). The experimentally obtained rejection results are compared to the simulated ones for the membrane model with interlayer distance of 0.70 nm (Fig. 8). While the simulation results underestimate the rejection of Zn(II) and Cd(II), they show good alignment with the experimental membrane regarding Pb(II) rejection. The discrepancy in separation performance likely arises from the experimental membrane containing ~ 500 times more GO layers than the model. Thus, the membrane with an interlayer distance of 0.70 nm would achieve complete rejection of Pb(II) cations.

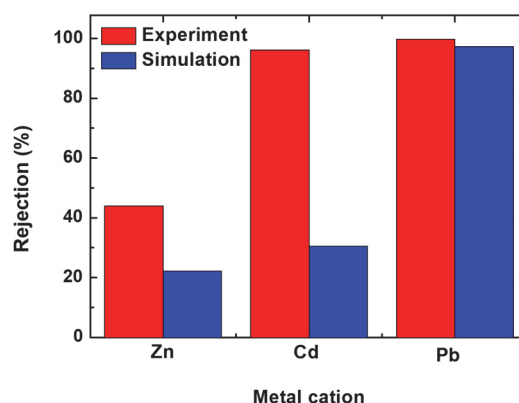


Fig. 8. Rejection against the metal cation for simulated and experimental membrane. We selected the interlayer distance of 0.70 nm for the membrane model because the experimental membrane had the similar interlayer distance, as determined from the XRD pattern using Bragg's law.

CONCLUSION

Landfill soil washing was conducted using H₂O and 0.01 M HCl under ultrasonication, yielding washed-off metal cations of Zn(II), Cd(II) and Pb(II). The soil's structure, determined to be the loam-type, remained similar after washing with both H₂O and 0.01 M HCl, suggesting that further development and enhancement of soil washing with water solvents are promising. The surface area of the loam-type soil increased to 235 m² g⁻¹ due to soil activation. The washed-off metal cations were filtered using a GO membrane prepared by vacuum filtration. The GO membrane reached rejections of 99.80, 96.15 and 44.00 % for Pb(II), Cd(II) and Zn(II), respectively. Water permeance showed a decreasing tendency from 20.3 to 7.8 L m⁻² h⁻¹ bar⁻¹ after 4 h of monitoring, which is due to membrane fouling by suspended particles in the leachate. This suggests that the membrane should be used in a series and replaced or washed frequently to achieve stable separations. Molecular dynamics (MD) simulations showed that ion separation occurs at the GO interfaces. Thus, we showed a possibility for a closed cycle of metal cation removal from the soil, which includes both soil washing and GO membrane implementation for metal cation separation.

SUPPLEMENTARY MATERIAL

Additional data and information are available electronically at the pages of journal website: <https://www.shd-pub.org.rs/index.php/JSCS/article/view/13361>, or from the corresponding author on request.

Acknowledgements. This project has received funding from the European Union's Horizon 2020 research and innovation programme under grant agreement no. 101007417 and from the taxpayers of the Republic of Serbia through the program grant number 451-03-137/2025-03/200134.

ИЗВОД

УКЛАЊАЊЕ Pb(II), Cd(II) И Zn(II) СА ЗЕМЉИШТА ДЕПОНИЈЕ И ПРОЦЕДНИХ ВОДА ПОМОЋУ ГРАФЕН-ОКСИДНЕ МЕМБРАНЕ

ДРАГАНА СТЕВИЋ¹, СУНЧИЦА СУКУР², РАДОВАН КУКОБАТ³, СУЗАНА ГОТОВАЦ АТЛАГИЋ², ПРЕДРАГ ИЛИЋ⁴, FRANCESCO SIRIO FUMAGALLI⁵, ANDREA VALSESIA⁵, PASCAL COLPO⁵ И СВЕТЛАНА ПОПОВИЋ¹

¹Технолошки факултет, Универзитет у Новом Саду, Булевар цара Лазара 1, Нови Сад, ²Природно-математички факултет, Катедра за хемију, Универзитет у Бањој Луци, Младена Стојановића 2, 78000, Бања Лука, Република Српска, Босна и Херцеговина, ³Технолошки факултет, Катедра за хемијско инжењерство и технологију, Универзитет у Бањој Луци, Булевар војводе Сидеје Сидејановића 73, Бања Лука, Република Српска, Босна и Херцеговина, ⁴Институт за заштитну и екологију Републике Српске, Бања Лука, Босна и Херцеговина и ⁵European Commission, Joint Research Centre (JRC), Ispra, Italy

Будући да кишница екстрахује токсичне метале из земљишта депонија формирајући штетне процедурне воде, потребно је развити методе за њихово уклањање. У раду је представљена метода уклањања токсичних металних јона из земље-иловаче, која се обухвата прање земљишта благим реагенсима за испирање, како би се издвојили метали у процедур

ној води, и пречишћавање процедурне воде филтрацијом кроз графен-оксид (GO) мембрану. Реагенси за прање H_2O и 0,01 M HCl су тестирани. GO мембрана је синтетисана користећи графит Мадагаскар. Раствор HCl је показао знатно већу ефикасност уклањања Pb(II), Cd(II) и Zn(II) него чиста вода захваљујући киселости. Чиста GO мембрана са растојањем између листова графена 0,68–0,74 nm (пре и после филтрације) и дебљине 0,70 μm је показала проценте одбијања 99,80 % за Pb(II), 96,15 % за Cd(II) и 44,00 % за Zn(II). Молекуларно-динамичка симулација је показала да се задржавање јона одвија на међуповршинама GO слојева, што је довело до прљања мембране. Ипак, високи проценти уклањања Pb(II) и Cd(II) јона указују на могућност пречишћавања процедурне воде земљишта депоније помоћу GO мембране.

(Примљено 5. маја, ревидирано 27. јуна, прихваћено 29. октобра 2025)

REFERENCES

1. G. Ondrasek, J. Shepherd, S. Rathod, R. Dharavath, M. I. Rashid, M. Brtnicky, M. S. Shahid, J. Horvatinec, Z. Rengel, *RSC Adv.* **15** (2025) 3904 (<https://doi.org/10.1039/D4RA04639K>)
2. D. Hou, X. Jia, L. Wang, S. P. McGrath, Y.-G. Zhu, Q. Hu, F.-J. Zhao, M.-S. Bank, D. O'Connor, J. Nriagu, *Science* **388** (2025) 316 (<https://doi.org/10.1126/science.adr5214>)
3. S. Sahragard, R. Mostafaloo, F. Fanaei, S. Imanian, M. Dehabadi, A. Adibzadeh, N. Nasseh, *Avicenna J. Environ. Health Eng.* **11** (2024) 115 (<https://doi.org/10.34172/ajehe.5467>)
4. S. M. Hosseini Beinabaj, H. Heydariyan, H. Mohammad Aleii, A. Hosseinzadeh, *Heliyon* **9** (2023) e13017 (<https://doi.org/10.1016/j.heliyon.2023.e13017>)
5. X. Zhai, Z. Li, B. Huang, N. Luo, M. Huang, Q. Zhang, G. Zeng, *Sci. Total Environ.* **635** (2018) 92 (<https://doi.org/10.1016/j.scitotenv.2018.04.119>)
6. K. N. B. Armel, B. B. B. Emile, A. K. Daniel, *J. Geosci. Environ. Prot.* **10** (2022) 151 (<https://doi.org/10.4236/gep.2022.101011>)
7. M.-S. Kim, N. Koo, J.-G. Kim, S.-H. Lee, *Appl. Sci.* **11** (2021) 6398 (<https://doi.org/10.3390/app11146398>)
8. K. Cho, E. Myung, H. Kim, C. Park, N. Choi, C. Park, *Int. J. Environ. Res. Publ. Health* **17** (2020) 3133 (<https://doi.org/10.3390/ijerph17093133>)
9. S. P. Bera, M. Godhaniya, C. Kothari, *J. Basic Microbiol.* **62** (2022) 245 (<https://doi.org/10.1002/jobm.202100259>)
10. G. Liu, W. Jin, N. Xu, *Chem. Soc. Rev.* **44** (2015) 5016 (<https://doi.org/10.1039/C4CS00423J>)
11. W. Jin, G. Liu, N. Xu, *Organic-Inorganic Composite Membranes for Molecular Separation*, Series on Chemical Engineering, Vol. 05, World Scientific (Europe), London, 2017 (<https://doi.org/10.1142/q0084>)
12. F. A. Janjhi, D. Janwery, I. Chandio, S. Ullah, F. Rehman, A. A. Memon, J. Hakami, F. Khan, G. Boczkaj, K. H. Thebo, *ChemBioEng Rev.* **9** (2022) 574 (<https://doi.org/10.1002/cben.202200015>)
13. A. Jeffers, *Soil Texture Analysis "The Jar Test."*, <https://hgic.clemson.edu/factsheet/soil-texture-analysis-the-jar-test/>
14. E. J. Coopersmith, B. S. Minsker, M. Sivapalan, *Hydrol. Earth Syst. Sci.* **18** (2014) 3095 (<https://doi.org/10.5194/hess-18-3095-2014>)
15. Z. Rengel, in *Soil Health and Climate Change*, B.P. Singh, A. L. Cowie, K. Y. Chan, K. Y., Eds., *Soil Biology*, Vol. 29, Springer, Heidelberg, 2011, pp. 69–85 (https://doi.org/10.1007/978-3-642-20256-8_4)

16. D. C. Marcano, D. V. Kosynkin, J. M. Berlin, A. Sinitskii, Z. Sun, A. Slesarev, L. B. Alemany, W. Lu, J. M. Tour, *ACS Nano* **4** (2010) 4806 (<https://doi.org/10.1021/nn1006368>)
17. R. J. Jiménez Riobóo, E. Climent-Pascual, X. Díez-Betriu, F. Jiménez-Villacorta, C. Prieto, A. De Andrés, *J. Mater. Chem., C* **3** (2015) 4868 (<https://doi.org/10.1039/C4TC02883J>)
18. A. P. Thompson, H. M. Aktulga, R. Berger, D. S. Bolintineanu, W. M. Brown, P. S. Crozier, P. J. In 'T Veld, A. Kohlmeyer, S. G. Moore, T. D. Nguyen, R. Shan, M. J. Stevens, J. Tranchida, C. Trott, S. J. Plimpton, *Comput. Phys. Commun.* **271** (2022) 108171 (<https://doi.org/10.1016/j.cpc.2021.108171>)
19. P. Mark, L. Nilsson, *J. Phys. Chem., A* **105** (2001) 9954 (<https://doi.org/10.1021/jp003020w>)
20. A. P. Rawat, V. Kumar, P. Singh, A. C. Shukla, D. P. Singh, *Soil Sediment Contam. Int. J.* **31** (2022) 15 (<https://doi.org/10.1080/15320383.2021.1900071>)
21. Z. Liu, W. Liu, X. Xie, W. Zhao, Y. Wen, Q. Wang, B. Ou, *IOP Conf. Ser. Earth Environ. Sci.* **252** (2019) 022022 (<https://doi.org/10.1088/1755-1315/252/2/022022>)
22. W. H. Bragg, W. L. Bragg, *Proc. R. Soc. London, A* **88** (1913) 428 (<https://doi.org/10.1098/rspa.1913.0040>)
23. B. Lee, K. Li, H. S. Yoon, J. Yoon, Y. Mok, Y. Lee, H. H. Lee, Y. H. Kim, *Sci. Rep.* **6** (2016) 28052 (<https://doi.org/10.1038/srep28052>)
24. M. Krishnamoorthy, M. Veerapandian, K. Yun, S.-J. Kim, *Carbon* **53** (2013) 38 (<https://doi.org/10.1016/j.carbon.2012.10.013>)
25. C. Ogata, M. Koinuma, K. Hatakeyama, H. Tateishi, M. Z. Asrori, T. Taniguchi, A. Funatsu, Y. Matsumoto, *Sci. Rep.* **4** (2014) 3647 (<https://doi.org/10.1038/srep03647>)
26. P. A. Khomyakov, G. Giovannetti, P. C. Rusu, G. Brocks, J. Van Den Brink, P. J. Kelly, *Phys. Rev., B* **79** (2009) 195425 (<https://doi.org/10.1103/PhysRevB.79.195425>)
27. R. Kukobat, M. Sakai, H. Tanaka, H. Otsuka, F. Vallejos-Burgos, C. Lastoskie, M. Matsukata, Y. Sasaki, K. Yoshida, T. Hayashi, K. Kaneko, *Sci. Adv.* **8** (2022) eabl3521 (<https://doi.org/10.1126/sciadv.abl3521>)
28. B. Mi, *Science* **343** (2014) 740 (<https://doi.org/10.1126/science.1250247>).